

# Recent Experiment Results during Electron Cyclotron Heating on HL-2A

Y.B.Dong, Yi Liu, H.J.Sun, Jun Zhou, W.W.Xiao, W.Chen, W.Deng,  
L.H.Yao, B.B.Feng, J.Rao, Q.W.Yang, X.T.Ding, Yong Liu, and  
C.H.Pan

*Southwestern Institute of Physics (SWIP), P.O Box 432, Chengdu 610041, China*

*E-mail of main author: [caroldyb@swip.ac.cn](mailto:caroldyb@swip.ac.cn)*

**Abstract.** The recent experiment results during electron cyclotron resonance heating (ECRH) on HL-2A tokamak are presented in this paper. During ECRH with a series of the supersonic molecular beam injection (SMBI) pulse fueling, the plasma storage energy  $W_E$ ,  $\beta_p$ , line averaged density  $n_e$  and “fusion neutron” count increase, leading to the plasma confinement improved. Furthermore, the non-local transport phenomena induced by SMBI have been firstly observed in HL-2A tokamak. The non-local effect induced by SMBI in HL-2A lasts much longer than that induced by pellet injection in other similar size tokamak; both the bolometer radiation and the  $H_a$  emission decrease when the non-local effect appears. It indicates that an electron transport barrier has possibly been formed at the position just outside the  $q = 1$  surface during this phase. In addition, the delayed core soft x-ray intensity decrease has been observed after ECRH switch-off, while the edge soft X-ray intensity decreases just after the ECRH switch off. The study shows transport coefficient reduces at all radii just after the off-axis ECRH switch off, especially near the heating deposition location. Moreover, various types of sawteeth activities during ECRH experiment are investigated, and the relationship between the sawtooth period and the power deposition location has been studied.

**Keywords:** electron cyclotron heating, non-local effect, ECRH switch-off, sawteeth activities.

**PACS:** 52.55.Fa; 52.50.Sw; 52.25.Fi; 52.35.Vd.

## INTRODUCTION

HL-2A is a divertor tokamak device with a major radius of 1.65m and a minor radius of 0.4m. The experiment was performed with line-averaged electron density  $n_e \sim 4.2 \times 10^{19} \text{m}^{-3}$ , central electron temperature  $T_e(0) \sim 5.0 \text{keV}$ , central ion temperature  $T_i(0) \sim 0.6 \text{keV}$ , plasma current  $I_p$  in the range 160–480 kA, toroidal magnetic field in the range 2.4–2.8 T[1]. ECRH is one of the main auxiliary heating schemes for the HL-2A plasma.

The ECRH system consists of two 68 GHz gyrotrons for fundamental resonance heating. In the present experiments, the ECRH/ECCD system with total power of 2 MW is realized and the electron temperature in central plasma of about 4.93keV has been achieved during ECRH. In the ECRH experiments, the direct response of plasma behaviors include electron temperature rising, and the electron density decreasing. The decrease may be related to the so-called density pump-out, which refers to the thermo-diffusive pinch in the particle flux at the application of ECRH to low density plasma [2].

In addition, a SMBI system has been further developed on the HL-2A for auxiliary fuelling [3]. Gas pressure is from 1MPa to 3MPa, and the pulse duration of jet is about 2 ms.

During ECRH with a series of pulse of SMBI fueling, the plasma storage energy  $W_E$ ,  $\beta_p$ , line averaged density  $n_e$  and “fusion neutron” count increase, the plasma confinement was improved, shown at Fig. 1.

This suggests that the injection of SMB weakens the outward heat diffusion. Further study will be conducted in the coming experiment in HL-2A. A new pneumatic supersonic molecular beam injector is developing to realize the SMBI from high-field side (HFS), which will be beneficial to deeper injection and higher fuelling efficiency.

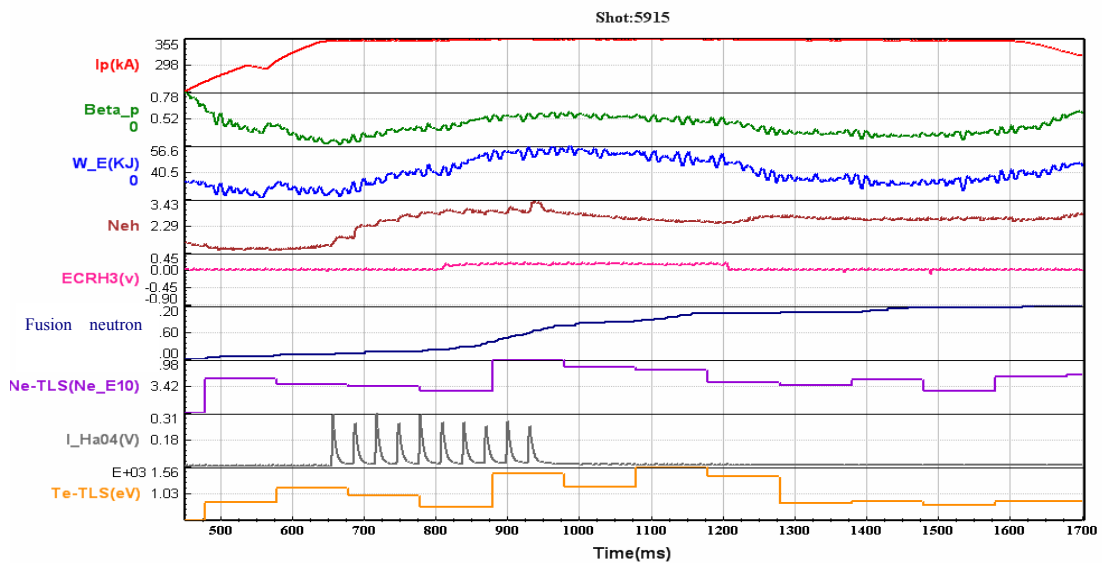


**FIGURE 1.** Confinement enhancement by SMBI during ECRH. (the plasma storage energy  $W_E$ ,  $\beta_p$ , line averaged density  $n_e$  and “fusion neutron” account increase. Ne-TLS and Te-TLS are the central density and temperature measured by the Tomson Laser Scattering(TLS) system. )

## NON-LOCAL PHENOMENA INDUCED BY SMBI

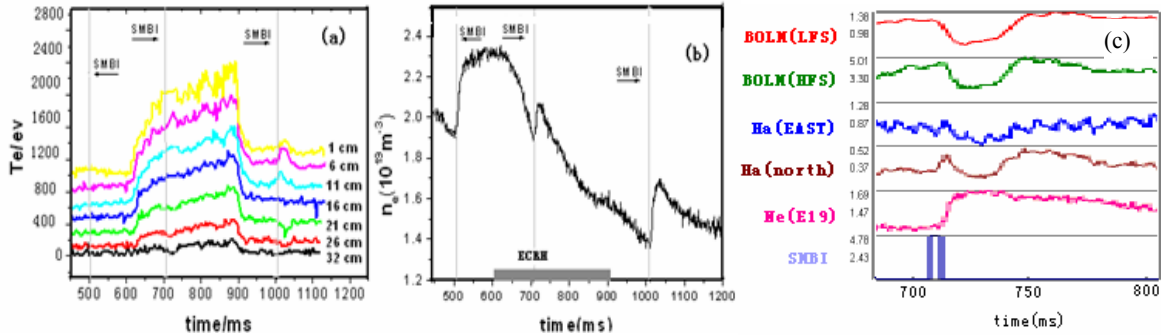


**FIGURE 2.** (a.) ECE  $T_e$  time traces at several radii with three SMBs injection before, during and after ECRH,  $B_t = 2.36$  T,  $I_p = 300$  kA,  $P_{\text{ECRH}} = 800$  kW. (b.) the line-averaged electron density time evolution (c.) the low field side bolometer, the high field side bolometer, the east  $H_\alpha$ , the north  $H_\alpha$ , the electron density, the SMBI signal.

From the first observation of the non-local transport phenomena at TEXT-U in 1995 [4], there are a few reports on many tokamaks [5, 6]. Such effect triggered by SMBI has been firstly observed on HL-2A tokamak. Three SMBs are respectively injected before ECRH, during ECRH and after ECRH, in order to investigate under what plasma condition the non-local effect occurs, as shown at Fig. 2(a). The non-local effect appears after the injection of the latter two SMBs, while the first one doesn't induce such an effect. After the second injection of SMB, outside  $r \sim 20$  cm the plasma is cooled by it while the core  $T_e$  increase. Central temperature increases 200eV. A steep  $T_e$  profile in the plasma core is sustained for about 40ms. The inverse position is several centimeters outside the  $q = 1$  surface, it is estimated that the position should be inside the  $q = 2$  surface. A strong dependence on plasma density is observed: the effect appears only in a low density plasma, around  $1.0 \times 10^{19} \text{ m}^{-3}$  and it disappears when then density is larger than  $2.0 \times 10^{19} \text{ m}^{-3}$ . The density before the injection of the first SMB almost equals to that of the second, the density before the last injection is much lower than the former two, in Fig. 2(b). It indicates that the effect always occurs with higher density during ECRH than OH case.

Furthermore, it was found that the bolometer radiation and  $H_\alpha$  emission decrease, indicating a total improvement of confinement, shown at Fig. 2(c), however, there is no sign of the decrease in the RTP tokamak. In addition, the effect induced by SMBI in HL-2A lasts much longer than that induced by pellet injection in other similar size tokamak: the duration of HL-2A is about 40 ms, while it is only 5 ms in RTP. Thus, the non-local effect is enhanced by SMBI in HL-2A, and an electron transport barrier has been formed at the position just outside the  $q = 1$  surface when the non-local effect

appears.

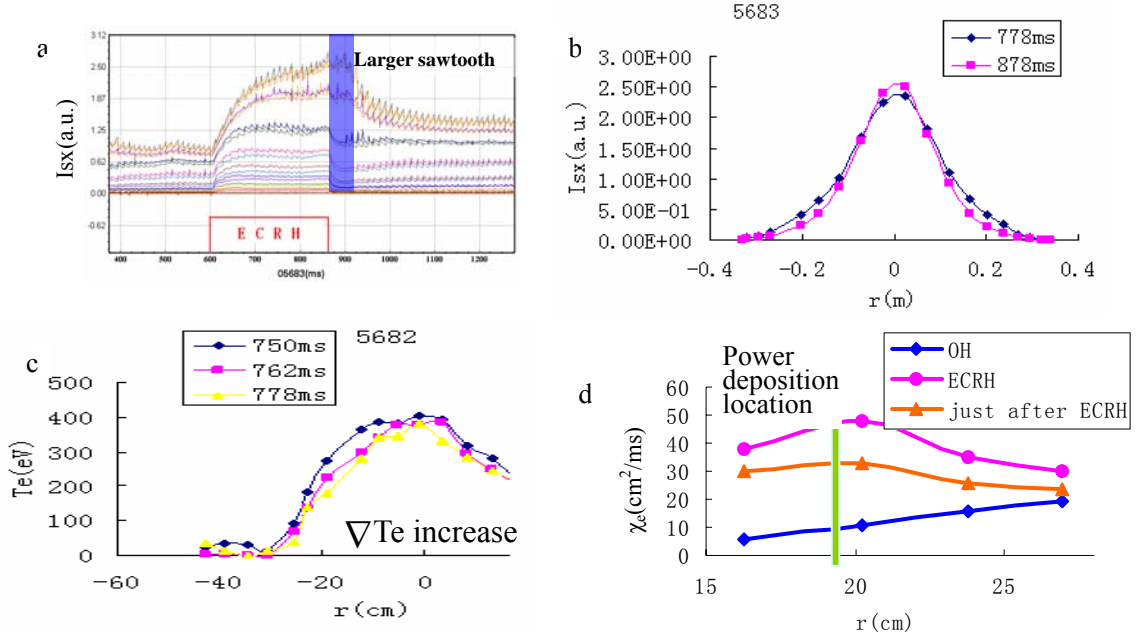


**FIGURE 3.** (a) Delayed decrease in the core  $I_{sx}$  after ECRH switch-off;  $B_t = 2.16$  T,  $I_p = 300$  kA,  $n_e = 2.6 \times 10^{19} \text{ m}^{-3}$ ,  $P_{\text{ECRH}} = 1100 \text{ kW}$ ; (b)  $I_{sx}$  profile during ECRH and after ECRH switch off; (c)  $T_e$  profiles before ECRH switch-off, 10 ms and 30ms after; (d) Electron heat diffusivity in the OH phase, at the end of the ECRH phase and just after the ECRH switch off.

## ITB TRIGGERED DURING ECRH

After the off-axis ECRH switch off, the core soft x-ray intensity does not decrease immediately. Instead, the core  $I_{sx}$  stays constant or even a slight increase for several tens of milliseconds before it starts to decrease, while the edge  $I_{sx}$  decreases just after the ECRH switch off (Fig. 3(a)). Thus a steep  $I_{sx}$  profile is formed (Fig. 3(b)), and the periods of sawteeth become larger. The  $\nabla T_e$  near the inverse surface increased during this phase, while  $\nabla n_e$  measured by microwave reflectometer increases slightly. Figure 3(d) shows the electron heat diffusivity in the OH phase, at the end of the ECRH phase and just after the ECRH switch off.

The value of  $\chi_e$  is larger during ECRH than OH discharge, and the maximum is observed near the heating deposition location. The transport coefficient reduces at all radii just after the off-axis ECRH switch off, especially near the heating deposition location. The possible explanation is that off-axis ECRH switch off leads to current density redistribution and transiently low magnetic shear near the rational magnetic surface causing the internal transport barrier (ITB) formation.

## SAWTEETH BEHAVIOUR DURING ECRH

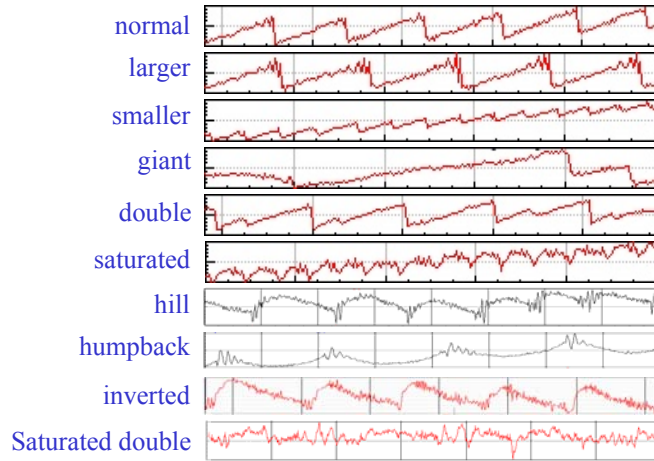


**FIGURE 4.** Various types of sawtooth activities during ECRH on HL-2A.

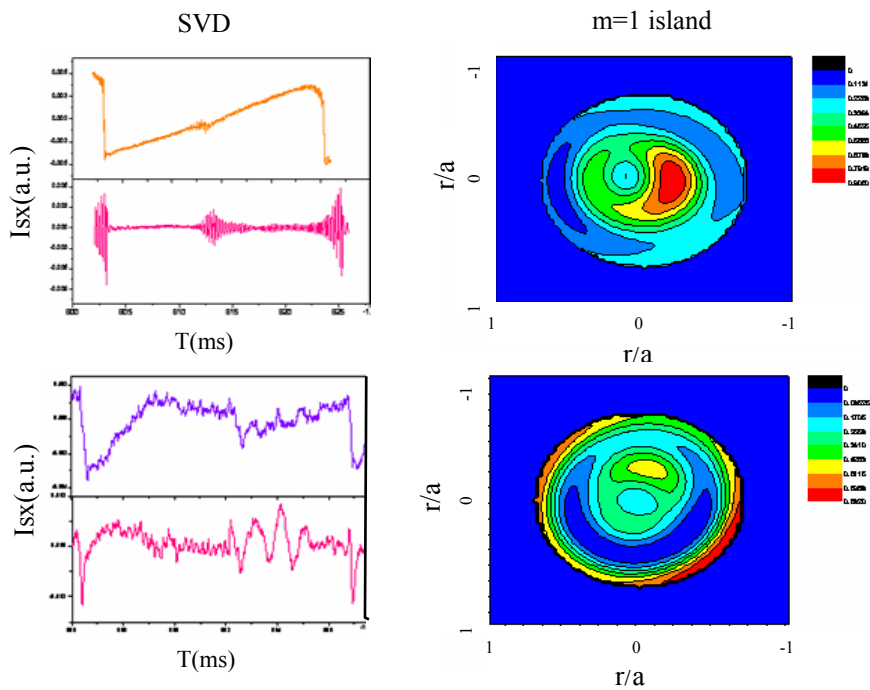


**FIGURE 5.** The SVD and tomography analysis results of double sawtooth and compound sawtooth

Compared with the sawteeth in Ohmic discharge, the sawteeth during ECRH tend to saturate or decrease in its ramp phase, and the sawteeth shapes are usually changed, leading to formation of a saturated sawtooth, an inverted sawtooth, a compound sawtooth, a humpback or a hill, as shown in Fig. 4. The saturated sawteeth always appear at lower ECRH power about 400-1080 kW, and inverted sawteeth appear at

higher ECRH, above 1100kW. Furthermore, with the increase of the central electron temperature in an ECRH discharge, the saturated sawteeth change into the inverted sawteeth.

These indicate that there are strong correlation between the central electron temperature and the propagation of magnetic reconnection during sawteeth crash phase. However, there is no evidence about the correlation between heating location and the change of the sawteeth phase on our tokamak. This result is different from that of the TCV tokamak[7]. The double sawteeth appear when the heating near the  $q = 1$  surface and both central disruptions in a cycle are due to magnetic reconnection associated with islands formed about  $q = 1$  surfaces. The saturated double sawteeth during the high central heating also include two crashes, but the difference is that the middle crash of double humpback sawtooth happens not during the rise ramp but the declivous ramp. From the singular value decomposition method (SVD) and tomography analysis shown at Fig. 5, it is obviously that the magnetic structures of both sawteeth are quite different, especially the  $m = 1$  island of the double sawtooth is bigger and hotter. It indicates that there is a strong effect of ECRH on sawtooth tailoring and magnetic reconnection in the vicinity of the  $q = 1$  surface.

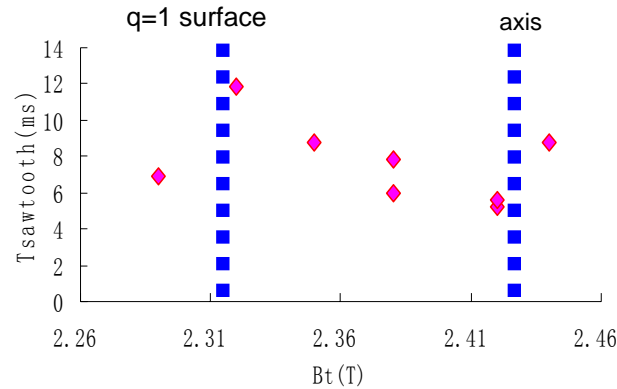


**FIGURE 6.** The relationship between the sawtooth period and the power deposition location.

The sawteeth stabilization has been observed in two ways: one is to increase the sawtooth period by heating close to the sawtooth inversion surface; another is to decrease the sawtooth period such as the hill sawtooth. Figure 6 shows the relationship between the sawtooth period and the power deposition location. The maximum sawtooth period is obtained for power deposition close to the HFS  $q = 1$  surface. The sawtooth periods are smaller near the axis.

The effect of localized ECRH on the local conductivity profile gives variation in the current penetration time in the core and hence shortens the current penetration time over the central region in the sawtooth ramp phase, leading to sawteeth with smaller periods. Such effect of ECH is qualitatively validated by the HL-2A discharges.

## SUMMARY

Some experimental results have been obtained in recent ECRH experiment on HL-2A tokamak. The most important conclusions are summarized as follows. Enhanced confinement is achieved by the SMBI during ECRH. Experimental results show that the injection of SMB weakens the inward propagation of the cold pulse and the outward heat diffusion. In addition, the enhanced non-local effect of edge cooling has been induced by the injection of SMB in the ECRH regime and the ohmic regime. It suggests that an electron transport barrier has been probably formed at the position just outside the  $q = 1$  surface and plasma confinement has been improved after the appearance of the non-local effect. Furthermore, the delayed  $I_{sx}$  decrease has been observed after the off-axis ECRH switch off. It is hypothesized that off-axis ECRH switch off leads to current density redistribution and a small shear near the rational magnetic surface causing the formation of an internal transport barrier. Lastly, we analyze the changes in the sawtooth activities during electron cyclotron heating, finding the strong effect of ECRH on the sawtooth tailoring and the magnetic reconnection in the vicinity of the  $q = 1$  surface.

## REFERENCES

1. Q. W. Yang, et al., Nucl. Fusion, 47 (2007) S635-S644.
2. A. G. Peeters, et al., Nucl. Fusion, 45 (2005) 1140.
3. L. H. Yao, et al., Nucl. Fusion, 41 (2001) 817.
4. K. W. Gentle, et al., Phys. Plasmas, 4 (1997) 3599.
5. M. W. Kissick, et al., Nucl. Fusion, 38 (1998) 821.
6. P. Mantica, et al., Phys. Rev. Lett, 82 (1999) 5048.
7. I. Furno, et al., Nucl. Fusion, 41 (2001) 403.